18

Electroporation of *Kluyveromyces marxianus* and β-D-galactosidase Extraction

Airton Ramos[1] and Andrea Lima Schneider[2]
[1]*State University of Santa Catarina*
[2]*University of Joinville*
Brazil

1. Introduction

Nowadays electroporation is well established as a method for increasing the permeability of biological membranes aiming to include some kind of molecule inside cells (anticancer drugs, for example) or to extract molecules from cells (enzymes, DNA, etc.). The permeabilized cells show a distribution of hydrophilic pores with diameters of several nanometers in the regions where the induced transmembrane potential rises above a threshold value from 200 mV to 1 V (Hibino *et al*, 1993; Teissie & Rols, 1993). The pore density and their diameters are dependent on the stimulation conditions: field strength, waveform and duration of stimulus (Weaver & Chizmadzhev, 1996; Teissié *et al*, 2005; Miklavčič & Puc, 2006; Chen *et al*, 2006)

Some previous studies have demonstrated experimentally the possibility of enzyme extraction from yeast by electroporation. Galutzov and Ganev (Galutzov & Ganev, 1999) investigated the extraction of glutathione reductase, 3-phosphoglicerate kinase e alcohol dehydrogenase from *Saccharomyces Cerevisiae* by electroporation. They used sequences of electric field pulses with strength 275 kV/m and duration of 1 ms. They observed increase in concentration of enzymes in the supernatant to about 8 hours after exposure to the field. The extraction efficiency was higher compared to other methods with mechanical or chemical lyses. Treatment with dithiothreitol before exposure to the field accelerated the extraction of glutathione reductase and alcohol dehydrogenase. This effect was considered to be related to the increased porosity of the cell wall due to the break of disulfide bonds in the layers of mannoproteins.

Ganev *et al* (Ganev *et al*, 2003) developed and used an electroporation system to stimulate a flow of yeast suspension up to 60 mL/min. They obtained the extraction of hexokinase, 3-phosphoglicerate kinase and 3-glyceraldehyde phosphate dehydrogenase from *Saccharomyces Cerevisiae*. They found that the maximum extraction is obtained after 4 hours with 15 pulses of frequency 6 Hz, but similar results were obtained for different combinations of field strength between 270 and 430 kV/m and pulse duration between 1 and 3 ms, so that stronger fields require shorter pulse to produce the same result in the extraction. The activity of enzymes extracted by electroporation was about double of those extracted by enzymatic and mechanical lysis of cells.

The extraction of β-D-galactosidase has a great interest due to its use in food and pharmaceutical industries. This enzyme is responsible for hydrolysis of lactose, disaccharide of low sweetness present on milk, resulting in its monosaccharide glucose and galactose. Its industrial importance is the application in dairy products for the production of foods with low lactose content, ideal for lactose intolerant consumers by improving the digestibility of milk and dairy. This is an important issue since lactase deficiency is present in about two thirds of the adult population worldwide, mainly in developing countries (Swagerty *et al*, 2002). In addition, lactase allows getting better technological characteristics and improves sensory and rheological properties of dairy products. Increase the power and sweetness that reduces the addition of sucrose, reducing the calorie content of foods. The formation of monosaccharides in dairy products helps in the metabolism of yeast fermented products. Lactase also reduces the probability of occurrence of the Maillard reaction, as galacto-oligosaccharides obtained did not act as reducing sugars.

The enzyme extraction method based on cell membrane permeabilization by electric field pulses applied to a suspension of yeast has advantages over chemical and mechanical methods due to its simplicity, efficiency in the extraction and preservation of enzyme activity and the cell itself, depending on the stimulation conditions. This study aims to evaluate the relationship between the change in membrane conductance during electrical stimulation of the cells and the enzyme β-D-galactosidase activity released by cells and to determine the stimulation conditions that maximize the extraction of this enzyme from *Kluyveromyces marxianus* yeasts.

The electroporation dynamics (opening and closing pores) is not completely understood. Part of this problem is because the electroporation is evaluated by indirect measurements (Kinosita & Tsong, 1979; He *et al*, 2008; Saulis *et al*, 2007). A number of methods have been used in the study of electroporation based on electrical measurements (Kinosita & Tsong, 1979; Huang & Rubinsky, 1999; Kotnik *et al*, 2003; Pavlin *et al*, 2005; Pliquett *et al*, 2004; Ivorra & Rubinsky, 2007; Suzuki *et al*, 2011). Electrical measurements and modeling were used to evaluate the effectiveness of electroporation in individual cells (Koester *et al*, 2010; Haque *et al*, 2009), cell suspensions (Kinosita & Tsong, 1979; Pavlin *et al*, 2005; Suzuki *et al*, 2011) and tissues (Grafström *et al*, 2006; Ivorra & Rubinsky, 2007; Laufer *et al*, 2010).

The membrane conductance after electroporation is related to electrical conductivity of cell suspension. Models are developed for isolated spherical or spheroidal cells using proposed membrane conductance distributions (Kinosita & Tsong, 1979; Pavlin & Miklavcic, 2003) and are obtained from the static solution to Laplace's equation using the simplest possible structure of a cell with a nonconductive thin membrane filled internally by a homogeneous medium. More complex situations in which the interaction between cells is not neglected or when the membrane conductance is calculated based on dynamic models of electroporation can be solved by numerical methods (Neu & Krassowska, 1999; Ramos *et al*, 2004; Ramos, 2010).

Conductivity measurement have been used in previous studies in order to determine the variation of the membrane conductance during electroporation (Kinosita & Tsong, 1979; Pavlin *et al*, 2005; Suzuki *et al*, 2011). But, caution is needed when using this approach. The impedance of the electrode interface with the suspension has strong dispersion of reactance and resistance at low frequencies, up to about 1 kHz (McAdams *et al*, 1995). Ionic diffusion

inside double layer of cells also results in low-frequency dielectric dispersion. Additionally, interfacial polarization shows strong dispersion with relaxation times of less than 1 μs for cells of a few microns in diameter (Foster & Schwan, 1995). Due to the reactive and dispersive effects, the precise determination of the suspension conductivity cannot be done using instantaneous values of voltage and current with pulsed waveform, since the spectral content of these signals is very wide.

The heating of the electrolyte during the pulse application also affects the relationship of conductivity with the membrane conductance. The variation of conductivity due to power dissipation in an aqueous electrolyte can be estimated by $\Delta\sigma/\sigma=\alpha\sigma_o E^2\Delta t/\rho c$, where α is the temperature coefficient, ρ and c are respectively the density and specific heat of water, E is the electric field strength applied and Δt is the time length of the pulse. For an aqueous NaCl electrolyte with initial conductivity of 20 mS/m and field of 400 V/m (typical values in our experiments) the variation of conductivity is 1.53% per millisecond. Thus, for a time of 10 ms, we can estimate a contribution of about 15% of variation in the suspension conductivity due only to heating of the sample. The conductivity of the external medium can also vary due to the efflux of ions through the hydrophilic pores created in the cell membrane. The external conductivity increases while the internal conductivity decreases, changing the relationship between suspension conductivity and membrane conductance.

Simple estimates of conductivity by measuring the instantaneous current and voltage during the pulse application are not reliable for a correct evaluation of the membrane conductance. In order to accomplish this goal in this study we measure the electrical impedance of the sample in a wide range of frequencies before and after the pulse application. Using a delay of 60 seconds to measure the impedance after the pulse, the generated heat is allowed to dissipate through the metal electrodes into the air. Once the volume of the suspension is small (about 300 μL), we can predict that thermal effects are negligible after 60 seconds.

The analysis of the impedance spectra enables us to identify and separate the effects of dispersion at low frequencies. In addition, one can adjust the parameters of a dielectric dispersion model for interfacial polarization of cell suspensions to obtain estimates of cell concentration, internal and external conductivities and membrane conductance for both intact cells and electroporated cells.

2. Methods

2.1 Experimental method

Cells of yeast *Kluyveromyces marxianus* CBS 6556 were used in the electroporation experiments. The cells were grown in stirred flasks containing 0.5 L with 150 mL of Bacto peptone (2%), yeast extract (1%) and lactose (2%) at 30 °C for 12 hours and 150 rpm. The colonies in the stationary phase were then washed three times in distilled water and centrifuged each time for six minutes at 12,000 rpm in an Eppendorf centrifuge and finally re-suspended in distilled water.

Samples in the final suspension were observed and photographed under a Olympus CX31 microscope with attached camera Moticam 1000 and software Motic Images Plus 2.0. 120 cell diameter measurements were performed in six different colonies used in the enzyme

activity and electrical impedance assays. The average radius obtained was 4.87 μm with a standard deviation of 1.07 μm.

The electroporator used in the experiments consists of a differential power amplifier with a gain of 50 V/V and an arbitrary waveform generator implemented in LabView™ (National Instruments) triggering a PCI 6251 card (National Instruments). Figure 1 shows a schematic representation of the electroporator. A current meter probe using a LTSP 25-NP sensor (LEM Components) and a voltage probe using resistive dividers and an INA 111 amplifier (Burr Brown) was implemented and used to measure current and voltage applied to the sample. The signals from the probes were acquired by the program through the PCI 6251 card using 16-bit resolution and 500 kHz of sampling rate simultaneously with the generation of the applied voltage. The sample holder is made of a cylindrical tube of nylon covering two steel electrodes 0.02 m in diameter and 0.001 m in spacing. The sample of the yeast suspension is injected and removed from the space between electrodes using syringes. The volume stimulated in each pulse application is 311 μL. All experiments were performed at room temperature of 25 °C. For each experiment, the electroporator was configured to generate an output voltage pulse from 100 to 400 Volts with duration from 1 to 10 ms.

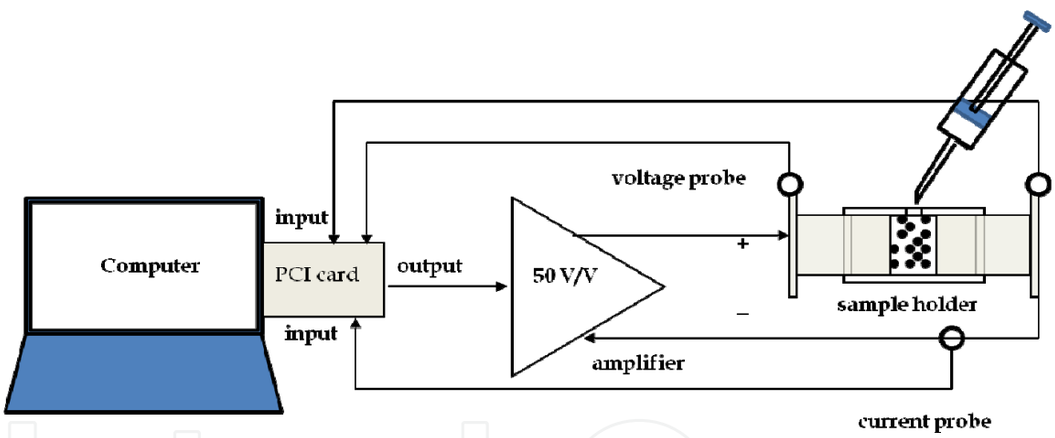

Fig. 1. Schematic of the electroporator

The enzyme activity assays were made 4 hours after pulsation. The cells were centrifugated for six minutes at 12,000 rpm in an Eppendorf centrifuge. To the supernatant was assigned the fraction of enzyme suspended outside the cells; to the pellets were assigned the enzyme associated to the cell walls. The cromogen ONPG, described by Lederberg (Lederberg, 1950) was used as a substrate. The assay mixture contained 780 μL sodium/phosphate buffer with pH 7.6 (containing 47 mM 2-mercaptoethanol and 1mM $MgCl_2$), 110 μL 35 mM ONPG and 110 μL of the enzyme solution. After one minute of incubation in a Thermomixer (Eppendorf) at 30º C, the reaction was stopped by 0.22 mL 1M Na_2CO_3. One unit (U) of β-galactosidase is defined as the amount of enzyme that releases 1 μmol of orto-nitrophenolate per minute under the assay conditions. This can be evaluated by means of measuring the increase of absorbance at 405 nm in a LKB spectrophotometer, using 1 cm optic path glass cuvettes. The molar extinction coefficient used was 3.1 μmol^{-1} cm^2 (Furlan *et al*, 2000).

The electrical impedance of the sample was measured before and after electroporation pulsation. We used a 4294A impedance analyzer (Agilent Technologies) in the range 40 Hz to 40 MHz. The time interval between the pulse application and the second measurement was kept in 60 seconds for all samples. This time is needed to allow disconnecting the sample holder from electroporator and connecting to the impedance analyzer as well as to allow the impedance reading to stabilize.

2.2 Mathematical method

The dispersion model for interfacial polarization in suspensions of spherical cells is obtained from Maxwell-Wagner theory of dispersion. For spherical particles of complex conductivity γ_c suspended in a medium of complex conductivity γ_o and occupying a volume fraction p, the following relationship applies between these quantities and the complex conductivity of the suspension γ_s (Foster & Schwan, 1995):

$$\frac{\gamma_s - \gamma_o}{\gamma_s + 2\gamma_o} = p\frac{\gamma_c - \gamma_o}{\gamma_c + 2\gamma_o} \tag{1}$$

Where $\gamma_c = \sigma_c + j\omega\varepsilon_c\varepsilon_o$, $\gamma_o = \sigma_o + j\omega\varepsilon_w\varepsilon_o$ and $\gamma_s = \sigma_s + j\omega\varepsilon_s\varepsilon_o$. In these equations ω is the angular frequency, ε_o is the vacuum permittivity, σ_c, σ_o and σ_s are the conductivities of cells, external medium and suspension, respectively, and ε_c, ε_w and ε_s are the dielectric constant of cells, water and suspension, respectively. The complex conductivity of cells can be estimated using the simple model consisting of a homogeneous internal medium with conductivity $\gamma_i = \sigma_i + j\omega\varepsilon_w\varepsilon_o$ surrounded by a spherical membrane of thickness h much smaller than the radius R and with complex conductivity $\gamma_m = h\left(G_m + j\omega C_m\right)$, where G_m and C_m are the conductance and capacitance per unit area of membrane, respectively. The result obtained after making approximations that keeps only terms of first order in (h/R) is the following (Foster & Schwan, 1995):

$$\gamma_c \cong \frac{\gamma_i + (2h/R)\gamma_m}{1 + (h/R)\left(\gamma_i - \gamma_m\right)/\gamma_m} \tag{2}$$

Substituting (2) in (1), the resulting expression can be separated into first order dispersion equations for the process of interfacial polarization at the cell membrane surface. The general expressions for the conductivity and dielectric constant of the suspension are written below:

$$\sigma_s = \sigma_{so} + \frac{\omega^2\tau_m^2\Delta\sigma_s}{1 + \omega^2\tau_m^2} \tag{3}$$

$$\varepsilon_s = \varepsilon_\infty + \frac{\Delta\varepsilon_s}{1 + \omega^2\tau_m^2} \tag{4}$$

$$\Delta\sigma_s = \frac{\varepsilon_o\Delta\varepsilon_s}{\tau_m} \tag{5}$$

In these equations, σ_{so} and ε_∞ are respectively the low frequency conductivity and high frequency dielectric constant of the suspension. $\Delta\sigma_s$ and $\Delta\varepsilon_s$ are the dispersion amplitudes of conductivity and dielectric constant, respectively, and τ_m is the relaxation time for interfacial polarization. Based on the model described by equations (1) and (2), the dispersion parameters of the first order equations (3) and (4) are presented below (Foster & Schwan, 1995):

$$\Delta\varepsilon_s = \frac{9pRC_m}{4\varepsilon_o\left[1+\frac{p}{2}+\frac{RG_m}{\sigma_i\sigma_o}\left(2\sigma_o+\sigma_i+p\left(\sigma_o-\sigma_i\right)\right)\right]^2} \tag{6}$$

$$\sigma_{so} = \sigma_o\left[\frac{1-p+\frac{RG_m}{\sigma_i\sigma_o}\left(\sigma_o+\frac{\sigma_i}{2}+p\left(\sigma_i-\sigma_o\right)\right)}{1+\frac{p}{2}+\frac{RG_m}{\sigma_i\sigma_o}\left(\sigma_o+\frac{\sigma_i}{2}-\frac{p}{2}\left(\sigma_i-\sigma_o\right)\right)}\right] \tag{7}$$

$$\tau_m = RC_m\frac{\sigma_i+2\sigma_o-p(\sigma_i-\sigma_o)}{2\sigma_i\sigma_o(1+p)+RG_m\left[\left(\sigma_i+2\sigma_o\right)-p\left(\sigma_i-\sigma_o\right)\right]} \tag{8}$$

The numerical method is initially applied to the parameterization of the impedance model of the sample. By considering the geometry of the electrodes with parallel faces and with radius much larger than the spacing, the following expression adequately represents the sample impedance:

$$Z_m = \frac{R_{ct}}{1+(j\omega\tau_e)^\beta}+\frac{d/A}{\sigma_s+j\omega\varepsilon_s\varepsilon_o} \tag{9}$$

Where A and d are the area and spacing of the electrodes, respectively. The first term in the second member represents the impedance of the electrode-electrolyte interface (McAdams *et al*, 1995). The second term is the impedance of the suspension. The parameters of the interface impedance model are: the charge transfer resistance R_{ct}, the surface relaxation time τ_e and the constant β. In the suspension impedance model the parameters to be obtained are shown in equations (3) and (4): σ_{so}, ε_∞, $\Delta\sigma_s$ or $\Delta\varepsilon_s$ and τ_m.

The parameterization algorithm used is based on successive approximations. Initially, each parameter is assigned a range of search. The parameters are stored in integer variables with 16 bits of resolution. Each interval is divided into 2^{16}-1 = 65,535 subintervals. The approximation process is performed by calculating all the answers of the equation (9) for a given parameter that varies throughout its subintervals, keeping the other parameters fixed at initial values. The value that minimizes the mean square error between the model and the measured impedance spectrum is selected. The process is repeated for all parameters, while maintaining the selected values of the parameters already adjusted. After several cycles of this procedure, the parameters of the model specified in equation (9) converge to the desired response. The convergence with mean square error less than 1% of the mean square value of

the impedance magnitude was achieved on average with 10 cycles of calculation. Figure 2 shows the result of the parameterization for an assay with applied field of 200 kV/m and time length of 10 ms. The obtained parameters are shown in the figure.

Using the values of σ_{so}, $\Delta\sigma_s$, $\Delta\varepsilon_s$ e τ_m obtained from the impedance spectrum measured before electroporation, the volume fraction p and membrane capacitance were calculated. In this case, the membrane conductance is very small, usually between 1 and 10 S/m² (Foster & Schwan, 1995) and the terms containing G_m in equations (6) to (8) can be neglected. Accordingly, these equations can be rewritten in the approximate forms:

$$\Delta\varepsilon_s = \frac{9pRC_m}{\varepsilon_o(2+p)^2} \tag{10}$$

$$\sigma_{so} = 2\sigma_o\frac{(1-p)}{2+p} \tag{11}$$

$$\tau_m = \frac{RC_m}{2\sigma_o}\frac{(1-p)}{(1+p)} \tag{12}$$

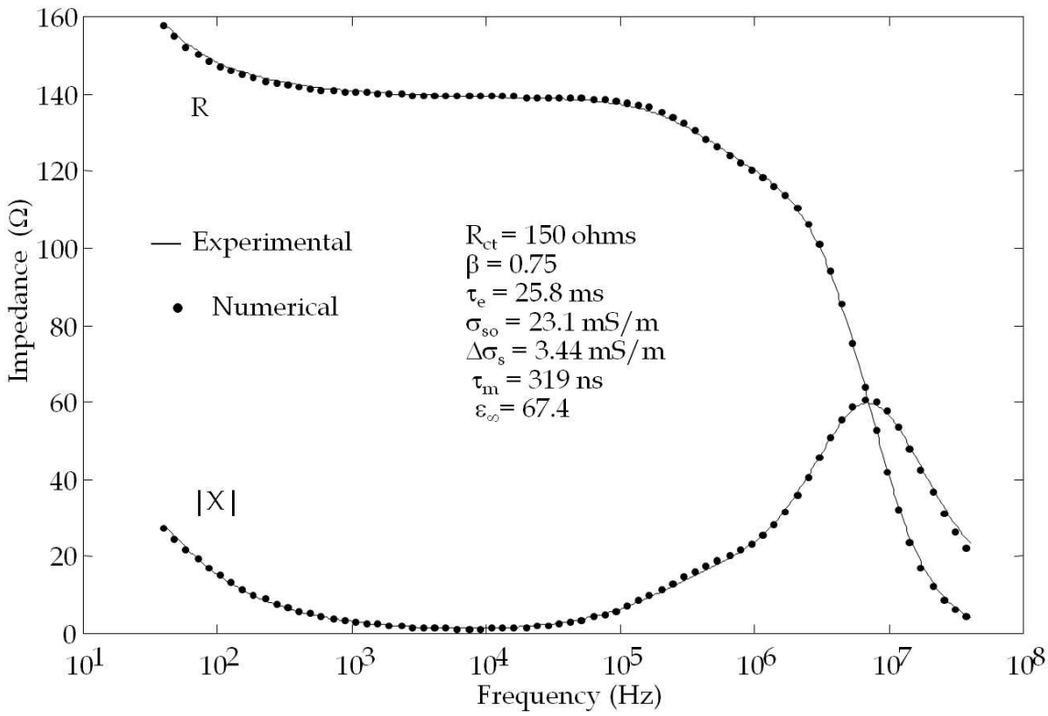

Fig. 2. Experimental and Theoretical impedance spectra to an assay with 200 kV/m and 10 ms. R – resistance; |X| modulus of reactance.

For the equation (12) it was assumed that $\sigma_i >> \sigma_o$, since the final suspension is obtained by diluting the cells in distilled water. Combining these equations with equation (5), we obtain an equation for calculating the volume fraction from σ_{so} e $\Delta\sigma_s$:

$$\frac{\Delta\sigma_s}{\sigma_{so}} = 9\frac{p(1+p)}{(2+p)(1-p)^2} \tag{13}$$

With the value of p in equation (10) yields the membrane capacitance C_m. Using the values of σ_{so}, $\Delta\sigma_s$, $\Delta\varepsilon_s$ and τ_m obtained from the impedance spectrum measured after electroporation, the membrane conductance and internal and external conductivities were calculated. Newton's method was used for this purpose. Defining the following variables: $x_1=RG_m$, $x_2=1/\sigma_i$ e $x_2=1/\sigma_o$, equations (6), (7) and (8) can be written in the respective forms:

$$F_1 = a_1 + 2a_1x_1x_2 + 2a_1a_2x_1x_3 - 1 = 0 \tag{14}$$

$$F_2 = b_1x_3 + b_1x_1x_2x_3 + b_1b_3x_1x_3^2 - x_1x_2 - b_2x_1x_3 - 1 = 0 \tag{15}$$

$$F_3 = c_1 + c_1c_2x_1x_3 + c_1c_3x_1x_2 - c_2x_3 - c_3x_2 = 0 \tag{16}$$

Where the coefficients are given in the Table 1 below.

$a_1 = \sqrt{\frac{\varepsilon_o\Delta\varepsilon_s(2+p)}{9pRC_m}}$	$a_2 = \frac{1-p}{2+p}$	———
$b_1 = \sigma_s\frac{(2+p)}{2(1-p)}$	$b_2 = \frac{(1+2p)}{2(1-p)}$	$b_3 = a_2$
$c_1 = \frac{\tau_m}{RC_m}$	$c_2 = \frac{(1-p)}{2(1+p)}$	$c_3 = \frac{(2+p)}{2(1+p)}$

Table 1. Coefficients of the dispersion equations for applying Newton's method.

Applying Newton's method the convergence was obtained in five steps with $\left\|[F_1F_2F_3]\right\|_\infty < 10^{-10}$ using the initial values: $G_m = 1000$ S/m², $\sigma_i = 500$ mS/m e $\sigma_o = 20$ mS/m.

3. Results and discussion

3.1 Impedance measurement

Each electroporation experiment was performed by applying a single pulse of electric field with strength 100, 200, 300 and 400 kV/m and time length from 1 to 10 ms. Figure 3 shows the typical behavior of the apparent conductance of the sample during electrical stimulation. These curves were obtained as the ratio between the voltage and current measured in the sample during the pulse application. This ratio is named apparent conductance because the sample actually has complex impedance with frequency dependent resistance and reactance. Since the applied pulse has a wide range of spectral components, it is not possible to obtain the conductance of the medium simply by dividing the instantaneous voltage and

current in the sample. In any case, the initial apparent conductance increases with the applied field, indicating the occurrence of electroporation. The slope of each curve also indicates that electroporation increases during the pulse. For more intense pulses the conductance shows greater variation. For intense fields, however, the heating of the sample is appreciable and this contributes to increase the sample conductance. Some authors, in previous studies, used instantaneous measurements of voltage and current for conductivity calculation and deduced the membrane conductance from these measurements (Kinosita & Tsong, 1979, Pavlin et al, 2005; Suzuki et al, 2011). It may indeed have a special interest in this approach since it would allow an assessment of the electroporation dynamics (pore opening rate) during application of the pulse. However, without an adequate measurement technique, the results may be adversely affected by other effects, such as the surface impedance of the electrodes and dielectric dispersion due to ion diffusion and accumulation on cell surface.

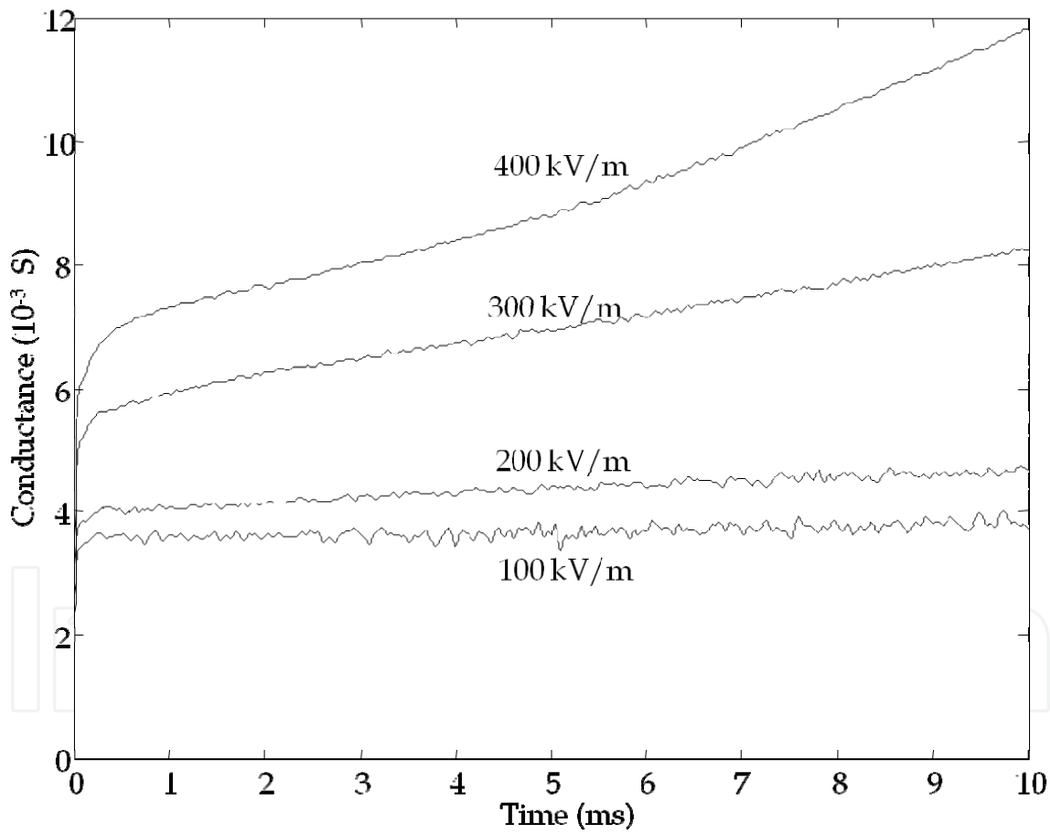

Fig. 3. Apparent sample conductance during the electroporation pulse with strength from 100 to 400 kV/m and time length of 10 ms.

A measurement technique that can be used to compensate for the reactive effects is the technique of small signals. In this case, one can use a small amplitude sinusoidal signal added to the electroporation pulse. This signal can be used to measure the change in conductance of the sample during the pulse. If the small-signal frequency is sufficiently far

from the dispersion band of the medium, the sample behaves like a real conductance and the conductivity obtained can be properly related to the variation of the membrane conductance. According to the impedance spectrum shown in Figure 2, the frequency of 10 kHz is adequate for this purpose. Another aspect to consider is the heating that results in increased conductivity of the electrolyte in the suspension. This effect seems to happen in the increase of the curve inclination for 400 kV/m in Figure 3 for pulse length higher than 5 ms. To avoid the interference of heating is necessary to limit the intensity of the applied field or the time length of the pulse.

Figure 4 shows the impedance spectra obtained before and after pulse application with 10 ms and field strengths of 100, 200, 300 and 400 kV/m. There is a strong reduction of the resistance through the frequency range up to 10 MHz and a significant reduction of the reactance at high frequencies for fields greater than 100 kV/m. One can assign both variations to the increase in membrane conductance. However, another effect that decreases the electrical impedance is the efflux of ions from the cytoplasm through the pores created in the cell membrane. This process has little effect on the apparent sample conductance shown in Figure 3, because its time constant is of the order of several seconds (Pavlin et al, 2005), but significantly affects the sample impedance measured after 60 seconds from pulse application. Another process that can have an effect is the cell swelling due to water influx through the pores due to the osmotic pressure difference. This process has time constant of tens of seconds to mouse melanoma cells (Pavlin et al, 2005). In yeast the effect of osmotic pressure is possibly reduced by the presence of the cell wall. Furthermore, in the experiments conducted in this study due to the small volume fraction of the suspension (about 3%) and low conductivity of the external medium (about 20 mS/m), the effects of cell swelling in the impedance are small. The field of 100 kV/m possibly lies just above the threshold of electroporation for yeast. The effects are relatively small as can be seen in Figure 4. There was also a tendency of saturation in the sample impedance for intense fields, suggesting that a maximum permeation can be achieved for fields of the order 400 kV/m.

3.2 Suspension conductivity and membrane conductance

Electroporation assays were repeated three times in all conditions of stimulation with samples prepared using the same procedure described above. The mathematical method used allowed to obtain the volume fraction, the membrane capacitance and conductivity of the external medium before electroporation. The range of values obtained for the set of 72 samples showed small standard deviation. The results obtained are: $p = 0.0332 \pm 0.0011$, $C_m = 3.5 \times 10^{-3} \pm 2.8 \times 10^{-4}$ F/m^2 and $\sigma_o = 24.6 \pm 2.7$ mS/m. The low membrane capacitance over the typically reported value for animal cells (of the order of 10^{-2} F/m^2) probably is due to the effect of the ionic distribution in the cell wall on the outer surface of the cell membrane. The cell wall of yeasts consists of two main types of macromolecules, polysaccharides glucan and mannan-type and several proteins, forming a reticulated structure with a thickness much larger than the cell membrane. The electrostatic interactions between these molecules and ions carried to the membrane by an applied electric field determine the spatial distribution of charge different from that seen in cells devoid of cell wall. The cell wall can also act as a filter for the efflux of macromolecules through the pores of the cell membrane as will be seen in relation to enzyme activity in this study.

The mathematical method applied to electroporated suspensions allowed to determine the change in conductivity of the external medium and membrane conductance. Figure 5 shows the variation of conductivity obtained with the impedance measurement before and after 60 seconds of pulse application as a function of field strength and pulse length. Figure 6 shows the distribution of membrane conductance obtained in the same analysis. The two sets of values are very similar. The correlation between them is mainly due to the fact that both depend on the number and size of pores in the cell membrane created by the applied field. Ions leaving the cells through these pores increase the conductivity of the external medium. This increase is small for 100 kV/m because this field is only slightly above the electroporation threshold. But as the applied field increases, the efflux of ions is increased and also shows a dependence on the pulse length. The conductivity measurement of the external medium can be used as a reliable indicator of the permeation state, provided that the reactive and dispersive effects in the sample are properly compensated.

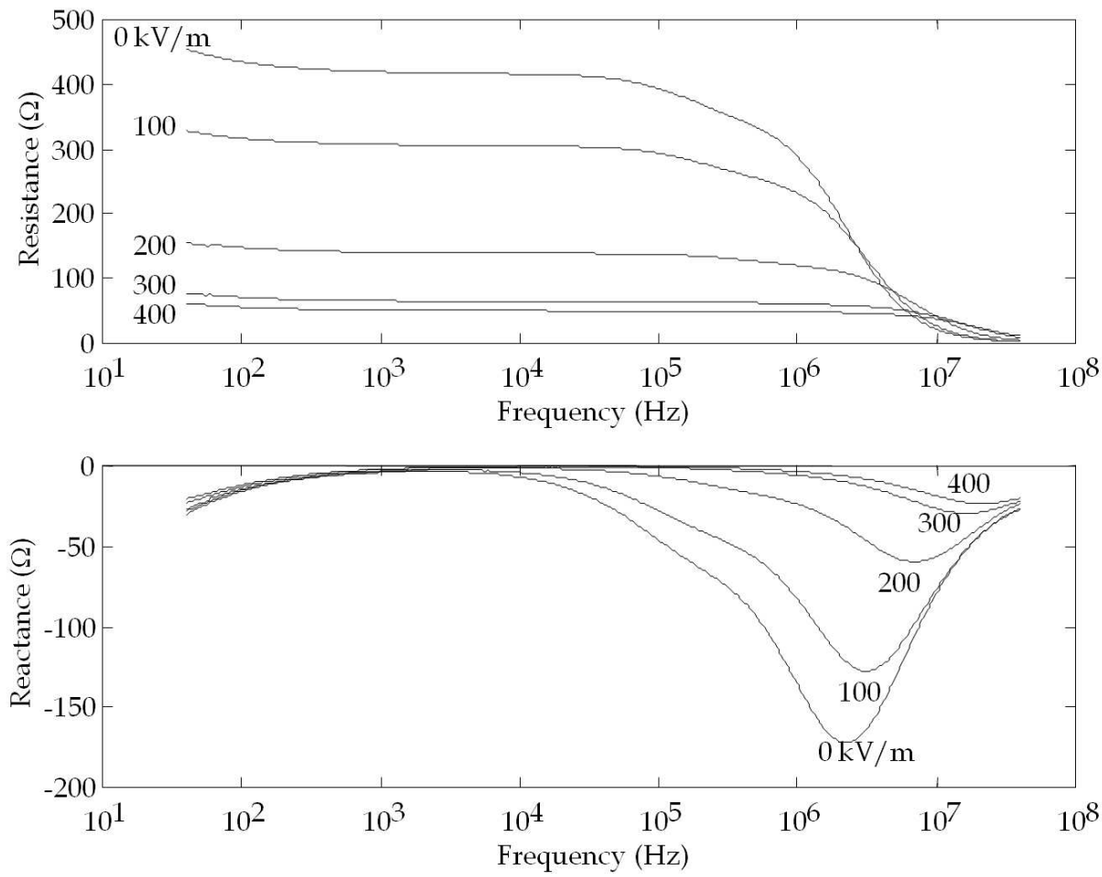

Fig. 4. Resistance and reactance obtained from the impedance spectra measured before (0 kV/m) and after (60 s) electroporation pulse with 10 ms and strength from 100 to 400 kV/m.

In Figure 6 the conductance increases rapidly with increasing applied field. The pulse length has increasing influence on membrane conductance as the applied field increases, but shows saturation for field of 400 kV/m and time length higher than 2 ms. The proposed models of

pore creation in electroporation are based on the Boltzmann statistical distribution that depends on the energy stored in the pores of the membrane (Glaser et al, 1988; Krassowska & Neu, 1999; Ramos, 2010). So these models have terms that depend exponentially on the squared transmembrane potential. It is expected therefore that the strength of the applied field has great influence on the change in membrane conductance, as shown in this figure. However, saturation of the conductance for intense fields means that the permeation state does not allow the transmembrane potential to grow indefinitely.

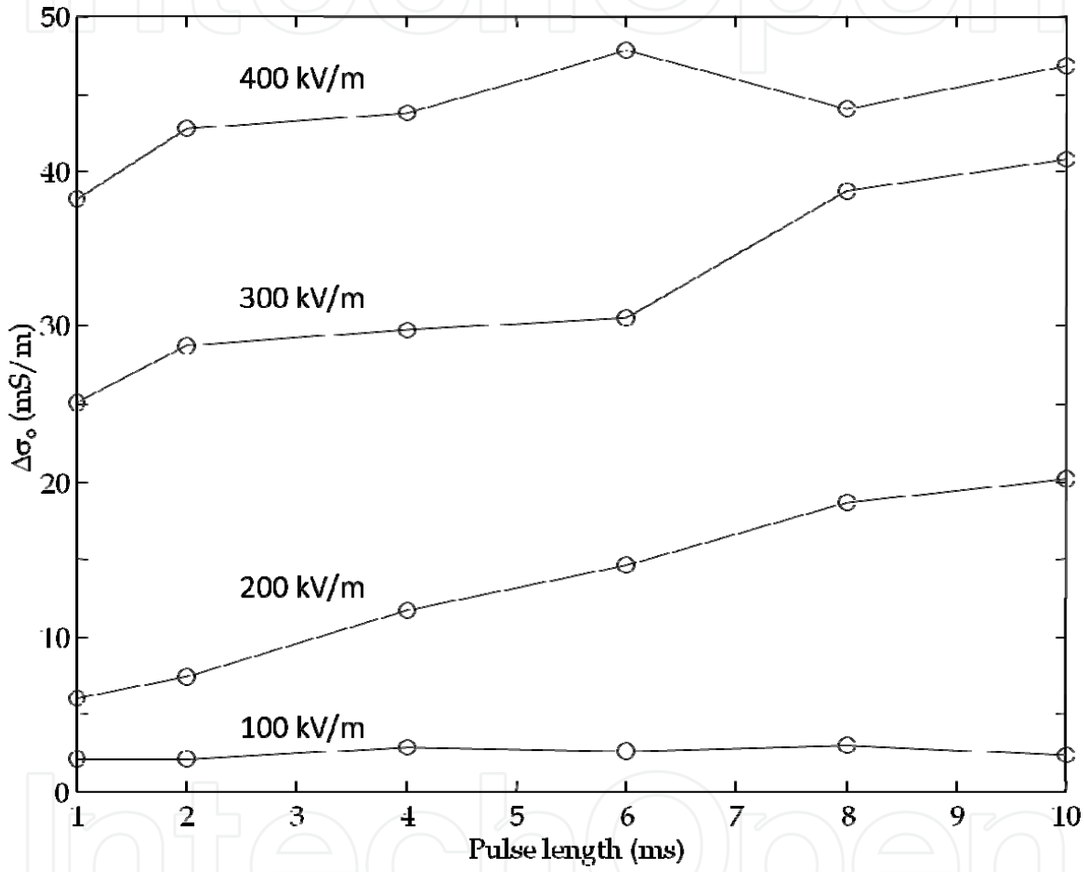

Fig. 5. Increase of external medium conductivity as a function of applied field strength and pulse duration.

Some previous studies with electroporation of animal cells resulted in very different membrane conductance values. Kinosita and Tsong (Kinosita & Tsong, 1979) used human red blood cells suspensions stimulated with single pulses of amplitude between 100 and 600 kV/m and duration up to 80 μs. They calculated the conductivity using instantaneous values and modeled the conductivity from a static solution to the electric potential internal and external to the cells. By fitting the model with the experimental results, they obtained conductance values of 10^5 and 10^6 S/m^2 to a field of 400 kV/m with duration of 2 and 80 μs, respectively. Human erythrocytes and the yeasts used in this study have different shapes but about the same size. However, the difference in the conductance obtained is big

compared to the results in Fig. 6. Possibly, there are significant influences of the conductivity measurement procedures and modeling method used. In addition, the cells in question are very different. As the erythrocyte has an oblate spheroid shape with axial ratio 0.28, the yeast is approximately spherical and the cell wall can play a role in reducing the transmembrane potential and membrane conductance. In the study by Pavlin *et al.* (Pavlin *et al*, 2005) mouse melanoma cells were electroporated with 8 pulses of electric field of the same amplitude and duration 100 μs each. The suspension conductivity was calculated using instantaneous values of voltage and current. They estimated the cell conductivity and membrane conductivity from numerical methods Membrane conductivity values obtained with a field of 84 kV/m were 3.5×10^{-5} S/m and 1.4×10^{-5} S/m for two medium conductivity, 1.58 S/m and 127 mS/m, respectively. Considering a membrane thickness of 5 nm, the membrane conductance is 7×10^{3} and 2.8×10^{3} S/m^2 respectively. The critical field for electroporation is probably lower for melanoma cells than for yeast, since the former are larger and do not have cell wall. The conductance values are within the order of magnitude as were obtained in this study.

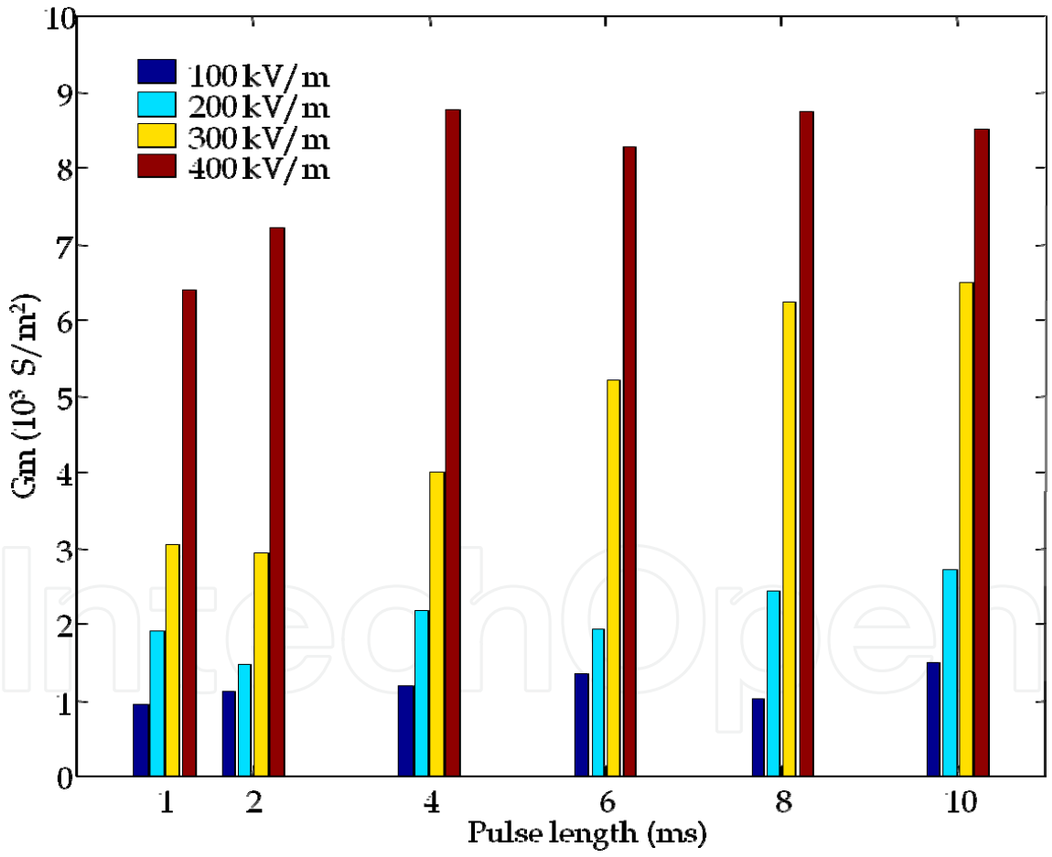

Fig. 6. Membrane conductance as a function of applied field strength and pulse duration.

3.3 Enzyme activity

Figure 7 shows the results of the β-D-galactosidase activity assays in suspensions electroporated with field strength from 100 to 400 kV/m and pulse length from 2 to 10 ms.

The fraction of enzyme activity found in the supernatant was very low in all trials. The values marked supernatant in the figure were obtained with field of 400 kV/m. The highest activity was detected in the cells themselves after centrifugation, indicating that although the enzyme is available outside the cell, it is not diluted in the supernatant. The enzyme is possibly trapped in the molecular network of the cell wall. Note that there is high correlation between the distributions of membrane conductance and enzymatic activity, especially above 200 kV/m. The enzymatic activity in the cell fraction for 400 kV/m is located just above 1 U for all pulse lengths in the same way that the conductance of the membrane shows saturation just above 8,000 S/m² for this field. Since the enzyme molecules must pass through the pores of the membrane to reach the cell wall, it can be predicted that the conditions that maximize the conductance of the membrane also maximize the extraction of the enzyme. The fact of the enzyme to be attached to the cell wall suggests an important application of the technique by means of immobilization. Cell immobilization consists in confinement of cells maintaining their catalytic activities. The enzyme β-D-galactosidase is not excreted naturally by the microorganism *Kluyveromyces marxianus*, but by electroporation it is possible to get it on the cell wall. Combining electroporation and cell immobilization is possible to obtain high catalytic activity in small volumes, provided that the cells remain viable after electrical stimulation and confinement.

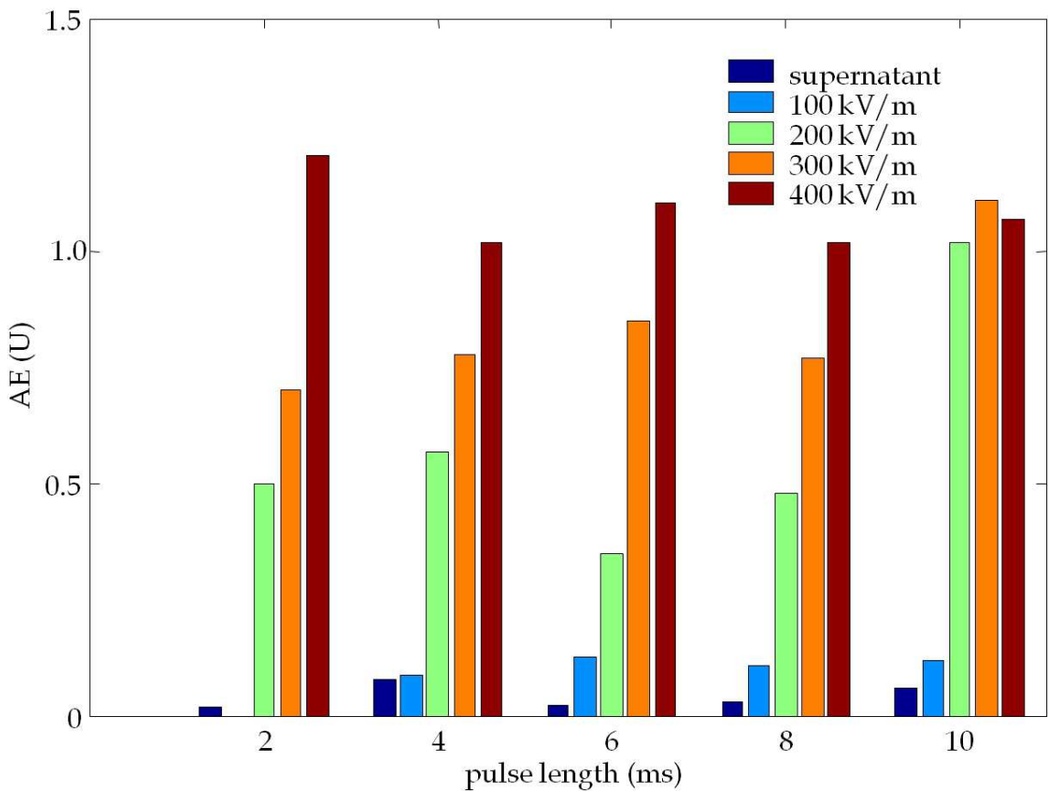

Fig. 7. Enzymatic activity for β-D-galactosidase in electroporated suspensions with fields strength from 100 to 400 kV/m and pulse length from 2 to 10 ms. The activity in the supernatant corresponds to the assay with 400 kV/m.

4. Conclusion

In this work it was studied the influence of the applied field strength and pulse duration on the increase in membrane conductance and activity of the enzyme β-D-galactosidase released by yeasts *Kluyveromyces marxianus* in suspension as a result of electroporation. The numerical technique for analyzing the electrical impedance spectra of the suspension has advantages over other modeling cited in the text because it allows properly compensate the reactive and dispersive effects caused by the impedance surface of the electrodes and ion accumulation on the cell membrane. It was found that membrane conductance and electrolyte conductivity measured after electroporation are strongly correlated, since both depend on the number and size of pores in the membrane. The protocol used with only a single pulse was able to produce large changes in membrane conductance for fields greater than 100 kV/m. The enzyme activity is also correlated to the membrane conductance. The membrane conductance increased between 8,000 and 9,000 S/m^2 for 400 kV/m. The enzyme activity was slightly greater than 1 U for all pulse duration. Both the membrane conductance and enzyme activity showed saturation for field of 400 kV/m, that is, the result is about independent on pulse length for pulses longer than 2 ms. The enzyme molecules after going through the pores in the cell membrane possibly get stuck in the molecular network of the cell wall. This was concluded based in the verification that the enzyme activity in the supernatant was very low in all assay conditions. Impedance measurement can allow the assessment of the permeation state of the membrane after pulse application, provided that the reactive and dispersive effects are properly modeled. This can be used as a probe for electroporation effectiveness evaluation aiming to control the enzyme extraction.

5. Future directions

Comparative studies with other methods of enzyme extraction, by chemical or mechanical process, should be conducted to determine the efficiency of electroporation compared to traditional techniques. The cell viability after electroporation also should be studied under different stimulation conditions, because it is an important factor to consider in certain applications. Another important study to conduct refers to the obtaining and using of immobilized enzymes on the cell wall of yeasts from electroporation process. The possibility of combining the technique of electroporation with the immobilization of enzymes appears promising but needs to be carefully tested and characterized.

6. References

Chen, C.; Smye, S.W.; Robinson, M.P. & Evans, J.A., (2006) Membrane Electroporation theories: a review, *Med. Biol. Eng. Comput.*, vol. 44, pp. 4-14

Foster, K.R. & Schwan, H.P. (1995) Dielectric properties of tissues, in: Handbook of Biological Effects of Electromagnetic Fields, Polk, C. & Postow, E. (Ed), 2ª Ed., pp. 25-102, CRC, New York

Furlan, S.A.; Schneider, A.L.S.; Merkle, R.; Carvalho, J.M.F. & Jonas R. (2000) Formulation of a lactose-free, low cost culture medium for the production of β–D-galactosidase by *Kluyveromyces marxianus*, *Biotechnology Letters*, vol. 22, pp. 589-593

Ganeva, V. & Galutzov, B. (1999) Electropulsation as an alternative method for protein extraction from yeast, *FEMS Microbiology Letters*, vol. 174, pp. 279-284

Ganeva, V.; Galutzov, B. & Teissie, J. (2003) High yield electroextraction of proteins from yeast by a flow process, *Analytical Biochemistry*, vol. 315, pp. 77-84

Glaser, R.W.; Leikin, S. L.; Chernomordik, L. V.; Pastushenko, V. F. & Sokirko, A. I. (1988) Reversible electrical breakdown of lipid bilayers: formation and evolution of pores, *Biochim. Biophys. Acta*, vol. 940, pp. 275-287

Grafström, G., Engström, P., Salford, L. G. & Persson, B. R. (2006) 99mTc-DTPA uptake and electrical impedance measurements in verification of *in vivo* electropermeabilization efficiency in rat muscle, *Cancer Biother.Radiopharm.*, vol. 21, pp. 623–635

Haque, A., Zuberi, M., Diaz-Rivera, R. E. & Porterfield, D. M. (2009) Electrical characterization of a single cell electroporation biochip with the 2-D scanning vibrating electrode technology, *Biomed Microdevices,* vol. 11, pp. 1239–1250

He, H., Chang, D. C. & Lee, Y. K. (2008) Nonlinear current response of micro electroporation and resealing dynamics for human cancer cells, *Bioelectrochemistry*, vol. 72, pp. 161-168.

Hibino, M.; Itoh, H. & Kinosita, Jr. K. (1993) Time courses of cell electroporation as reveled by submicrosecond imaging of transmembrane potential, *Biophysical Journal*, v. 64, pp. 1798-1800

Huang, Y. & Rubinsky, B. (1999) Micro-electroporation: improving the efficiency and understanding of electrical permeabilization of cells, *Biomed. Microdevices*, vol. 2, pp. 145–150

Ivorra, A. & Rubinsky, B. (2007) In vivo electrical impedance measurements during and after electroporation of rat liver, *Bioelectrochemistry*, v. 70, pp. 287–295

Kinosita, K. & Tsong, T.Y. (1979) Voltage-induced conductance in human erythrocyte membranes, *Bioch. Bioph. Acta*, vol. 554, pp. 479-497

Kotnik, T., Pucihar, G., Rebersek, M., Miklavcic, D. & Mir, L. M. (2003) Role of pulse shape in cell membrane electropermeabilization, *Biochimica et Biophysica Acta*, vol. 1614, pp. 193-200

Koester, P. J., Tautorat, C., Beikirch, H., Gimsa, J. & Baumann, W. (2010) Recording electric potentials from single adherent cells with 3D microelectrode arrays after local electroporation, *Biosensors and Bioelectronics*, vol. 26, pp. 1731-1735

Laufer, S., Ivorra, A., Reuter, V. E., Rubinsky, B. & Solomon, S. B. (2010) Electrical impedance characterization of normal and cancerous human hepatic tissue, Physiol. Meas., vol. 31, pp. 995-1009

Lederberg, J. (1950) The β-D-galactosidase of *Escherichia coli* strain K-12, *J. Bacteriol.* , vol. 60, pp. 381-392

McAdams, E.T.; Lackermeier, A.; McLaughlin, J.A.; Macken, D. & Jossinet, J. (1995) The linear and non-linear electrical properties of the electrode-electrolyte interface, *Biosensors & Bioelectronics*, vol. 10, pp. 67-74

Miklavčič, D. & Puc M. (2006) Electroporation, in: *Wiley Encyclopedia of Biomedical Engineering*, Akay M. (Ed), pp. 1-11, John Wiley & Sons Inc., New York

Neu, J.C. & Krassowska, W. (1999) Asymptotic model of electroporation, *Phys. Review E.*, vol. 59, pp. 3471-3482

Pavlin, M.; Kanduser, M.; Rebersek, M.; Pucihar, G.; Hart, F. X.; Magjarevic, R. & Miklavcic, D. (2005) Effect of cell electroporation on the conductivity of a cell suspension, *Biophysical Journal*, vol. 88, pp. 4378-4390

Pavlin, M. & Miklavcic, D. (2003) Effective conductivity of a suspension of permeabilized cells: A theoretical analysis, *Biophys. J.*, vol. 85, pp. 719-729

Pliquett, U., Elez, R., Piiper, A. & Neumann, E. (2004) Electroporation of subcutaneous mouse tumors by rectangular and trapezium high voltage pulses, *Bioelectrochemistry*, vol. 62, pp. 83–93

Ramos, A. (2010) Improved numerical approach for electrical modeling of biological cell clusters, *Med. Biol. Eng. Comput.*, vol. 48, pp. 311-319

Ramos, A., Suzuki D.O.H. & Marques J.L.B. (2004) Numerical simulation of electroporation in spherical cells, *Artificial Organs*, v. 28, pp. 357-361

Reed, S. D. & Li, S. (2009) Electroporation Advances in Large Animals, *Curr Gene Ther.*, vol. 9, pp. 316–326

Rice, J., Ottensmeier, C. H. & Stevenson, F. K. (2008) DNA vaccines: precision tools for activating effective immunity against cancer, *Nature Reviews Cancer*, vol. 8, pp. 108-120

Saulis, G., Satkauskas, S. & Praneviciute, R. (2007) Determination of cell electroporation from the release of intracellular potassium ions, *Analytical Biochemistry*, vol. 360, pp. 273-281

Sersa, G., Miklavcic, D., Cemazar, M., Rudolf, Z., Pucihar, G. & Snoj, M. (2008) Electrochemotherapy in treatment of tumours, *EJSO*, vol. 34, pp. 232-240

Suzuki, D. O. H.; Ramos, A.; Ribeiro, M. C. M.; Cazarolli, L. H.; Silva, F. R. M. B.; Leite, L. D. & Marques, J. L. B. (2011) Theoretical and Experimental Analysis of Electroporated Membrane Conductance in Cell Suspension, *IEEE Transactions on Biomedical Engineering*, *In press*

Swagerty, D.L.; Walling, A.D. & Klein, R.M. (2002) Lactose Intolerance, *Am Fam Physician*, vol. 65 (9), (Mai 1), pp. 1845-1851

Teissié, J.; Golzio, M.; & Rols M. P. (2005). Mechanisms of cell membrane electropermeabilization: A minireview of our present (lack of ?) knowledge, *Biochim. Biophys. Acta.*, vol. 1724, (Aug. 2005), pp. 270-280

Teissie, J. & Rols, M.P. (1993) An experimental evaluation of the critical potential inducing cell membrane electropermeabilization, *Biophysical Journal*, vol. 65, pp. 409-413

Weaver, J.C. & Chizmadzhev, Y. A. (1996) Theory of electroporation: a review, *Bioelectrochemistry*, vol. 41: pp. 135-160

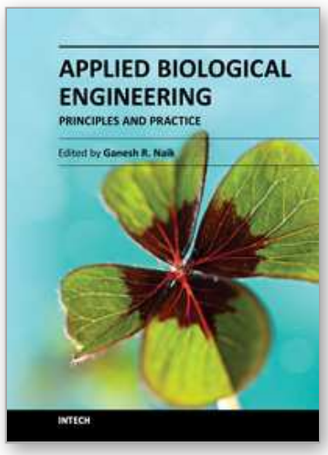

Applied Biological Engineering - Principles and Practice

Edited by Dr. Ganesh R. Naik

ISBN 978-953-51-0412-4
Hard cover, 662 pages
Publisher InTech
Published online 23, March, 2012
Published in print edition March, 2012

Biological engineering is a field of engineering in which the emphasis is on life and life-sustaining systems. Biological engineering is an emerging discipline that encompasses engineering theory and practice connected to and derived from the science of biology. The most important trend in biological engineering is the dynamic range of scales at which biotechnology is now able to integrate with biological processes. An explosion in micro/nanoscale technology is allowing the manufacture of nanoparticles for drug delivery into cells, miniaturized implantable microsensors for medical diagnostics, and micro-engineered robots for on-board tissue repairs. This book aims to provide an updated overview of the recent developments in biological engineering from diverse aspects and various applications in clinical and experimental research.

InTech Europe
University Campus STeP Ri
Slavka Krautzeka 83/A
51000 Rijeka, Croatia
Phone: +385 (51) 770 447
Fax: +385 (51) 686 166
www.intechopen.com

InTech China
Unit 405, Office Block, Hotel Equatorial Shanghai
No.65, Yan An Road (West), Shanghai, 200040, China
中国上海市延安西路65号上海国际贵都大饭店办公楼405单元
Phone: +86-21-62489820
Fax: +86-21-62489821

IntechOpen